## EXTENDED EXPERIMENTAL PROCEDURES

### Animal Studies

Male Sprague-Dawley rats (~400 g) were obtained from Charles River Laboratories. After the rats acclimated for at least one week, they underwent surgery under isoflurane anesthesia to place polyethylene catheters in the common carotid artery and jugular vein. Rats were fed normal chow (5% calories from fat, 18% protein, 77% carbohydrate) or a safflower oil-based high fat diet (HFD) (60% fat, 20% protein, 20% carbohydrate) for 2-28 days, as specified in the text, and were fasted overnight before each study.

Mice with knockout of Akt1 and Akt2 and Foxo1 were generated as described (Lu et al., 2012) and were fed regular chow. Mice with macrophage specific JNK knockout (Han et al., 2013) or adipose-specific ATGL knockout (Ahmadian et al., 2011; Haemmerle et al., 2006) were generated as described. Both groups were fed a lard-based high fat diet containing 60% calories from fat for 4 weeks. All mice underwent surgery to place a polyethylene catheter in the jugular vein. Mice were studied 7 days after surgery to allow adequate recovery before additional experiments were performed.

Insulin receptor was knocked down in rats using a single injection of a 2'-O-methoxyethyl chimeric antisense oligonucleotide (50 mg × $kg^{-1}$) from Isis Pharmaceuticals (Obici et al., 2002). Two days following the injections, rats underwent infusion studies as described below.

### Basal and Hyperinsulinemic-Euglycemic Clamp Studies

Mice were clamped as described (Jurczak et al., 2012). To measure whole-body lipolysis, they were co-infused with [U-$^{13}$C] sodium palmitate (300 mg•$kg^{-1}$•min-1) and [1,1,2,3,3-$d^5$] glycerol (2.25 μmol•$kg^{-1}$•$min^{-1}$) for the duration of the 120 min basal infusion. Blood was collected from the tail vein at 120 min and the mice were sacrificed by injection of sodium pentobarbital. Liver and white adipose tissue were freeze-clamped in tongs pre-cooled in liquid nitrogen within 10 and 30 seconds of euthanasia, respectively, and stored at −80°C for further analysis.

Mice used for clamp studies received a primed-continuous infusion of insulin as described (Jurczak et al., 2012), and were co-infused with [U-$^{13}$C] sodium palmitate and [1,1,2,3,3-$d^5$] glycerol at the rates listed above. Blood was collected from the tail for measurement of plasma glucose, insulin, and tracer at set time points during the 140-min infusion, and a variable infusion of 20% dextrose was given to maintain euglycemia. At 140 min, a final blood sample was collected and the mice were euthanized and tissues collected as described above.

Rats used for basal studies received a continuous infusion of [$^3$H] glucose (0.1 μCi/min) and [1,1,2,3,3-$d_5$] glycerol (1.5 μmol•$kg^{-1}$•$min^{-1}$) for 120 min. One milliliter of blood was taken through the venous catheter at the end of the study, and animals were sacrificed with intravenous sodium pentobarbital. Liver and white adipose tissue were collected as described above and stored at −80°C.

### Hepatic Flux Modeling

The contributions of glycerol and oxaloacetate (OAA) were measured in rats infused with [3-$^{13}$C] lactate (5 min prime 120 μmol/[kg-min], 115 min basal infusion 40 μmol x $kg^{-1}$ × $min^{-1}$) and [3-$^3$H] glucose (0.1 μCi × $min^{-1}$). After 120 min, rats were sacrificed with intravenous pentobarbital, and livers were immediately freeze-clamped in situ in tongs pre-cooled in liquid $N_2$. The positional $^{13}$C enrichment of liver glucose was measured as we have described (Perry et al., 2014), while the $^{13}$C malate enrichment was measured using LC/MS/MS. Whole-body glucose production was measured using the [3-$^3$H] glucose specific activity in plasma at steady-state (100-120 min) (Jurczak et al., 2012), with 90% of the measured glucose production assumed to come from the liver (Perry et al., 2014). The fractional contribution of oxaloacetate to gluconeogenesis was calculated using the formula $\frac{V_{GNG\ OAA}}{V_{GNG}} = \frac{^{13}C\ glucose_{1,2,3,4,5,6} + {}^{13}C_3\ glucose + {}^{13}C_4\ glucose}{2*{}^{13}C_{1,2,3,4}\ malate}$, with gluconeogenesis from glycerol assumed to comprise the rest of the measured gluconeogenesis.

### Measurement of Hepatic Acetyl CoA Concentrations

To measure hepatic acetyl CoA concentrations, ~100 mg liver tissue was homogenized in 1 mL ice cold 10% trichloroacetic acid. An internal standard (5 nmol [1,2-$^{13}C_2$] acetyl CoA and 5 nmol [$^{13}C_3$] malonyl CoA) was added before homogenization. The samples were mixed on a rotating shaker for 30 min at 4°C and centrifuged at 4000 g for 5 min at 4°C. The supernatant was then loaded on a C18 cartridge, which had been preconditioned by 3 mL HPLC-grade methanol, then 4 mL 1 mM HCl. After the supernatant flowed through the cartridge, it was washed with 3 mL 1 mM HCl and 1 mL distilled water. The flow-through was then discarded. Finally, acetyl CoA was eluted from the cartridge with 2 mL ethanol-water (65-35%, v/v) containing 0.1 M ammonium acetate followed by 2 mL 50% HPLC-grade methanol-water. The samples were dried in a Speed Vac for the minimum time necessary (~6 hrs), resuspended in 100 μL distilled water, and transferred to LC/MS/MS vials.

LC/MS/MS method development and analysis was performed on an Applied Biosystems 6500 QTRAP, equipped with a Shimadzu ultrafast liquid chromatography system using an electrospray ionization source with positive-ion detection. The quantitative analysis of the CoA metabolites was simultaneously monitored in MRM mode with $^{13}$C labeled metabolites (acetyl-1,2-$^{13}C_2$ CoA and malonyl-$^{13}C_3$ CoA) as the internal standards. A Varian C18 HPLC column (150 mm x 2 mm) was used to improve the sensitivity and to spread the peaks with an isocratic flow rate of 300 l × $min^{-1}$ of 15% methanol aqueous solution containing 10 mM ammonium acetate.

Acetyl CoA and [1,2-$^{13}C_2$] acetyl CoA were selectively monitored with the ion pairs of 810.0/303.1 and 812.0/305.1, respectively. Malonyl CoA and [$^{13}C_3$] malonyl CoA were selectively monitored with the ion pairs of 854.0/347.1 and 857.0/350.1, respectively. The optimized MS parameters were: curtain gas 35; collision gas med, ionization potential 4500 V, probe temperature 5000C; ion source gas 1 50; ion source gas 2 65; declustering potential 120 V; entrance potential 10 V. The collision energy (40-160 V) and collision cell exit potential (8-20 V) were found to be ion-pair-dependent, and they were optimized for each individual metabolite.

## Human Studies

As part of the Yale Pathophysiology of Type 2 Diabetes in Obese Youth Study study, all subjects underwent an oral glucose tolerance test and a detailed assessment of abdominal fat distribution by MRI. Sixty obese adolescents agreed to have a subcutaneous peri-umbillical adipose tissue biopsy and 49 of them underwent hyperinsulinemic-euglycemic clamp combined with infusions of [6,6-$^2H_2$] glucose and [1,1,2,3,3-$^2H_5$] glycerol to assess basal and insulin-stimulated rates of glucose and glycerol turnover respectively as previously described (Petersen et al., 2003). Their clinical characteristics are described in Table S1. Thirty-eight of these subjects completed a previous study (Kursawe et al., 2010). None of the subjects was on any medications nor had any known disease. The nature and potential risks of the study were explained to all subjects before obtaining their written informed consent. The study was approved by the Yale University Human Investigation Committee.

In the morning at 8 am, after an overnight fast of 10-12h, insulin sensitivity was measured with a hyperinsulinemic-euglycemic clamp during which time insulin was administered as a primed-continuous infusion of 80 mU/($m^2$•min) for 120 min and variable glucose was administered to maintain euglycemia.

Whole body composition was measured by dual-energy X-ray absorptiometry with a Hologic scanner (Boston, MA). Abdominal magnetic resonance imaging (MRI) studies were performed on a GE or Siemens Sonata 1.5 Tesla system. Five slices, obtained at the level of the L4/L5 disc space, were analyzed for each subject as previously reported (Cali et al., 2009).

One to two-gram samples of abdominal subcutaneous adipose tissue were obtained via surgical excision inferior to the umbilicus after administration of 0.25% lidocaine with adrenaline for local anesthesia. The mean diameter of large adipocytes was calculated as previously described (Kursawe et al., 2010).

Total RNA was isolated using TRIzol reagent and was further purified using an RNeasy kit (Qiagen, Valencia, CA). The quantification of several differentially expressed genes by real-time RT-PCR was performed using an ABI 7000 Sequence Detection System (Applied Biosystems). The nucleotide sequences of the primers and PCR conditions can be provided upon request. For each run, samples were run in duplicate for both the gene of interest and 18S. Quantitative analysis was determined by Δ/ΔCT method normalized to both a control and 18S message.

Abdominal subcutaneous biopsies from 42 subjects were used for immunohistochemical staining and CD68 was used as a marker for macrophages. Staining was performed using a standard protocol on sections from formalin-fixed paraffin-embedded tissue blocks. Serial sections were deparaffinized, rehydrated and treated with 10 mM citrate buffer (pH 6.0) in a steamer and then endogeneous peroxidase was blocked with 3% $H_2O_2$. The sections were then incubated for 1 h at room temperature with primary antibodies, mouse monoclonal anti-CD68 (Ab-3 clone KP1, Thermo Fisher Scientific). After rinsing in TBS buffer containing 0.25% Triton X-100 (pH 7.2), sections were incubated with ENVISION+ (K4007 or K4011, DAKO) followed by visualization with 3.3'-diaminobenzidine tetrachloride. All sections were counterstained with GILL III Hematoxylin, dehydrated and coverslipped with a resinous mounting media. For each subject, the number of macrophages (identified as CD68+ cells) within 10 regions of interest were counted by two independent observers using a light microscope and normalized to the number of counted adipocytes.

Plasma glucose levels were measured using the YSI 2700 STAT Analyzer (Yellow Springs Instruments) and lipid levels were measured using an Autoanalyzer (model 747-200, Roche-Hitachi). Plasma insulin was measured with a radioimmunoassay (Linco).

## SUPPLEMENTAL REFERENCES


Ahmadian, M., Abbott, M.J., Tang, T., Hudak, C.S., Kim, Y., Bruss, M., Hellerstein, M.K., Lee, H.Y., Samuel, V.T., Shulman, G.I., et al. (2011). Desnutrin/ATGL is regulated by AMPK and is required for a brown adipose phenotype. Cell Metab. *13*, 739–748.

Cali, A.M., De Oliveira, A.M., Kim, H., Chen, S., Reyes-Mugica, M., Escalera, S., Dziura, J., Taksali, S.E., Kursawe, R., Shaw, M., et al. (2009). Glucose dysregulation and hepatic steatosis in obese adolescents: is there a link? Hepatology *49*, 1896–1903.

Haemmerle, G., Lass, A., Zimmermann, R., Gorkiewicz, G., Meyer, C., Rozman, J., Heldmaier, G., Maier, R., Theussl, C., Eder, S., et al. (2006). Defective lipolysis and altered energy metabolism in mice lacking adipose triglyceride lipase. Science *312*, 734–737.

Jurczak, M.J., Lee, A.H., Jornayvaz, F.R., Lee, H.Y., Birkenfeld, A.L., Guigni, B.A., Kahn, M., Samuel, V.T., Glimcher, L.H., and Shulman, G.I. (2012). Dissociation of inositol-requiring enzyme (IRE1α)-mediated c-Jun N-terminal kinase activation from hepatic insulin resistance in conditional X-box-binding protein-1 (XBP1) knock-out mice. J. Biol. Chem. *287*, 2558–2567.

Petersen, K.F., Befroy, D., Dufour, S., Dziura, J., Ariyan, C., Rothman, D.L., DiPietro, L., Cline, G.W., and Shulman, G.I. (2003). Mitochondrial dysfunction in the elderly: possible role in insulin resistance. Science *300*, 1140–1142.

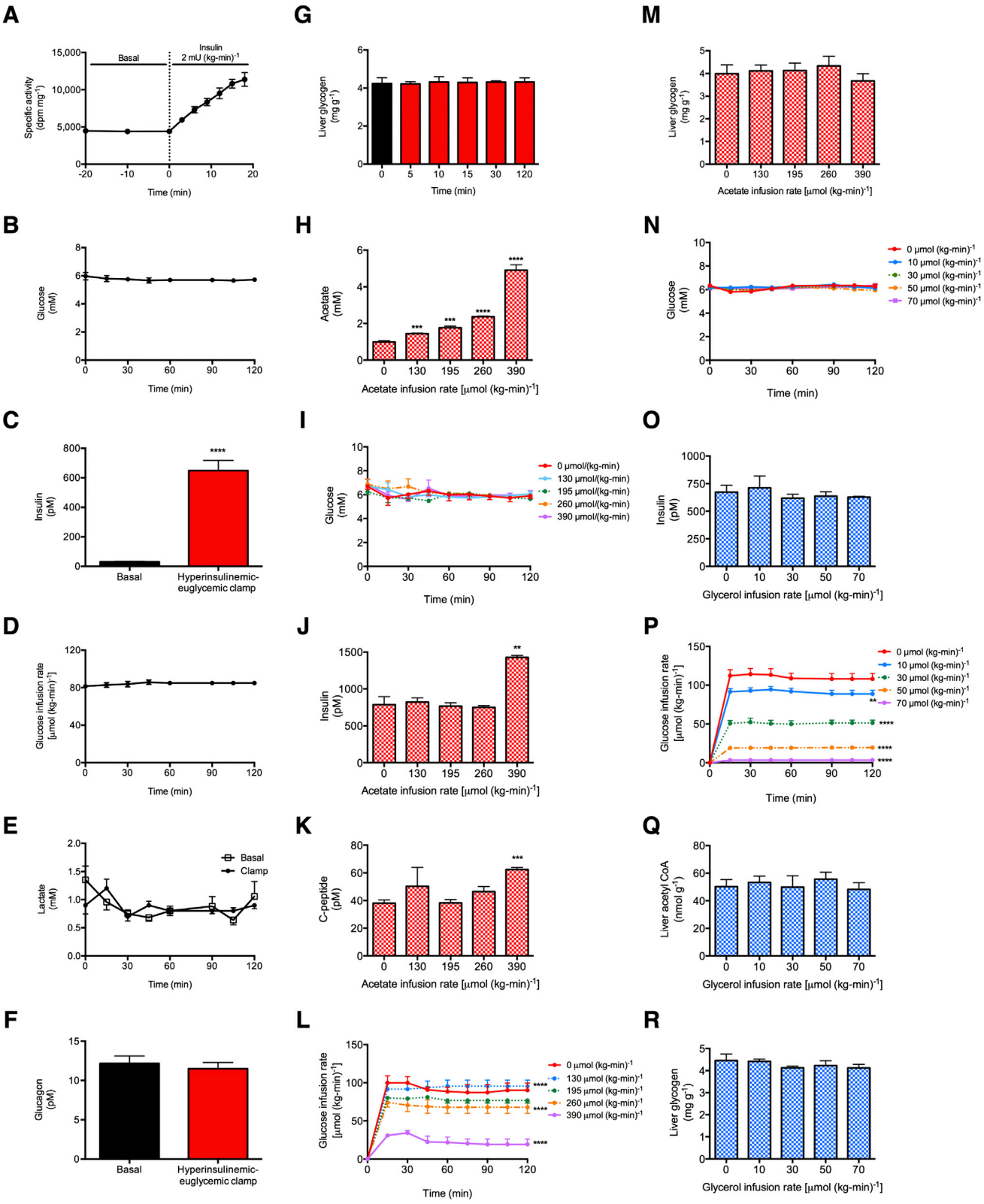


*(legend on next page)*

**Figure S1. Insulin Suppresses Gluconeogenesis within 10 Min by Suppressing Lipolysis and Reducing Hepatic Acetyl CoA Concentrations, Related to Figure 1**

(A) Plasma $^{3}$H glucose specific activity.
(B) Plasma glucose concentrations during a hyperinsulinemic-euglycemic clamp.
(C) Plasma insulin concentrations. ****p < 0.0001.
(D) Glucose infusion rate during the clamp.
(E) Plasma lactate concentrations during a basal infusion (open squares) or clamp (closed circles).
(F) Plasma glucagon concentrations.
In (A)-(F), n = 6 per group.
(G) Liver glycogen concentrations after varying periods of a hyperinsulinemic-euglycemic clamp.
(H) Plasma acetate concentrations during a clamp with co-infusion of acetate.
(I–K) Plasma glucose, insulin, and c-peptide concentrations.
(L) Glucose infusion rate.
(M) Liver glycogen content.
(N) Plasma glucose concentrations during a clamp with co-infusion of glycerol.
(O) Plasma insulin.
(P) Glucose infusion rate.
(Q) Liver acetyl CoA.
(R) Liver glycogen.
In (G–R), n = 4 per group or per time point. **p < 0.01, ***p < 0.001, ****p < 0.0001 versus 0 μmol/(kg-min) by the 2-tailed unpaired Student's t test. Data are mean ± SEM.

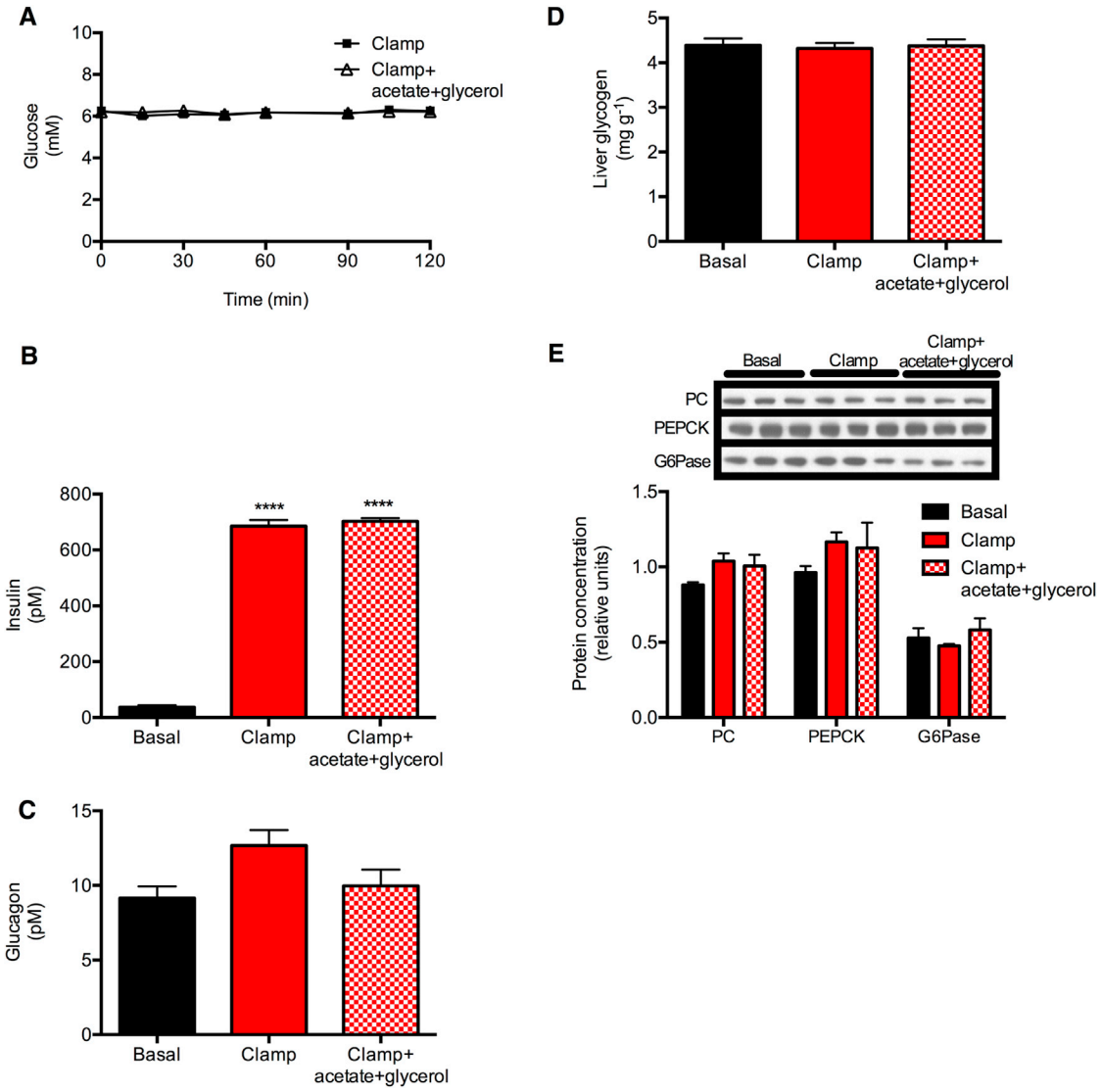


**Figure S2. Normalizing Hepatic Acetyl CoA Concentrations and Whole-Body Glycerol Turnover to Baseline Levels in the Hyperinsulinemic-Euglycemic Clamp Negates Insulin's Ability to Suppress Hepatic Glucose Production, Related to Figure 2**

(A) Plasma glucose concentrations.

(B) Plasma insulin concentrations. ****$p < 0.0001$ versus basal.

(C) Plasma glucagon.

(D) Liver glycogen.

(E) Liver gluconeogenic protein expression.

In all panels, data are mean ± SEM of n = 6 per group. Comparisons by ANOVA (B-E) or by t test (A).

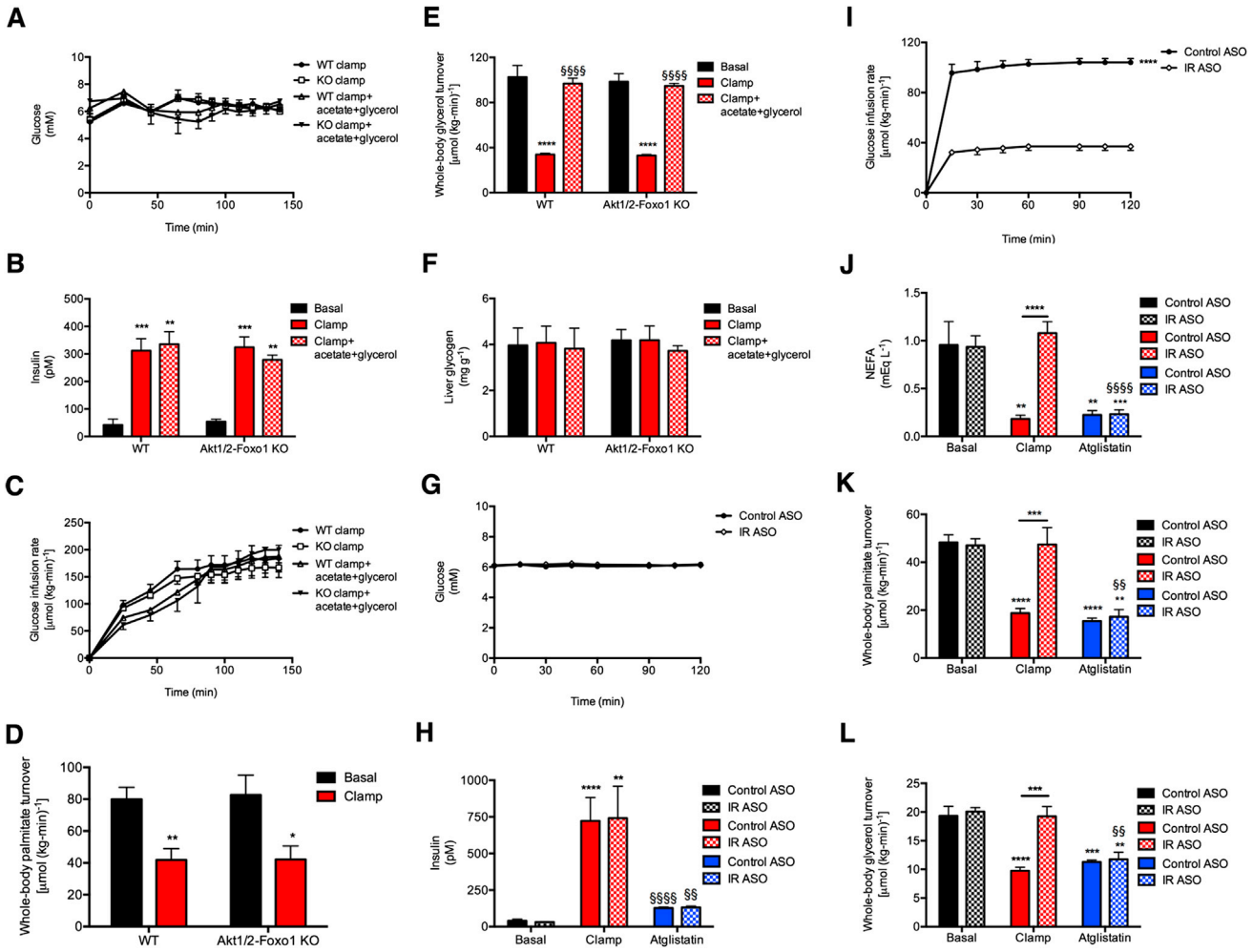


**Figure S3. Suppression of Lipolysis Results in Decreased Hepatic Acetyl CoA Concentrations and Suppression of Hepatic Glucose Production, Related to Figure 3**

(A) Plasma glucose during a hyperinsulinemic-euglycemic clamp.

(B) Plasma insulin. In (A–F), *p < 0.05, **p < 0.01, ***p < 0.001, ****p < 0.0001 versus basal; §§§§ p < 0.0001 versus clamp.

(C) Glucose infusion rate.

(D) Whole-body palmitate turnover.

(E) Whole-body glycerol turnover.

(F) Liver glycogen content. In (A–F), n = 5 per group (basal), 8-9 per group (clamp), or 3-4 per group (clamp+acetate+glycerol).

(G) Plasma glucose concentrations during a hyperinsulinemic-euglycemic clamp in rats with the insulin receptor knocked down in liver and WAT.

(H) Plasma insulin.

(I) Glucose infusion rate.

(J) Plasma NEFA concentrations.

(K) Whole-body palmitate turnover.

(L) Whole-body glycerol turnover.

In (G–L), **p < 0.01, ***p < 0.001, ****p < 0.0001 versus basal; §§ p < 0.01, §§§ p < 0.001, §§§§ p < 0.0001 by one-way ANOVA with Bonferroni's multiple comparisons test. In (G–L), data are mean ± SEM of n = 6 per group.

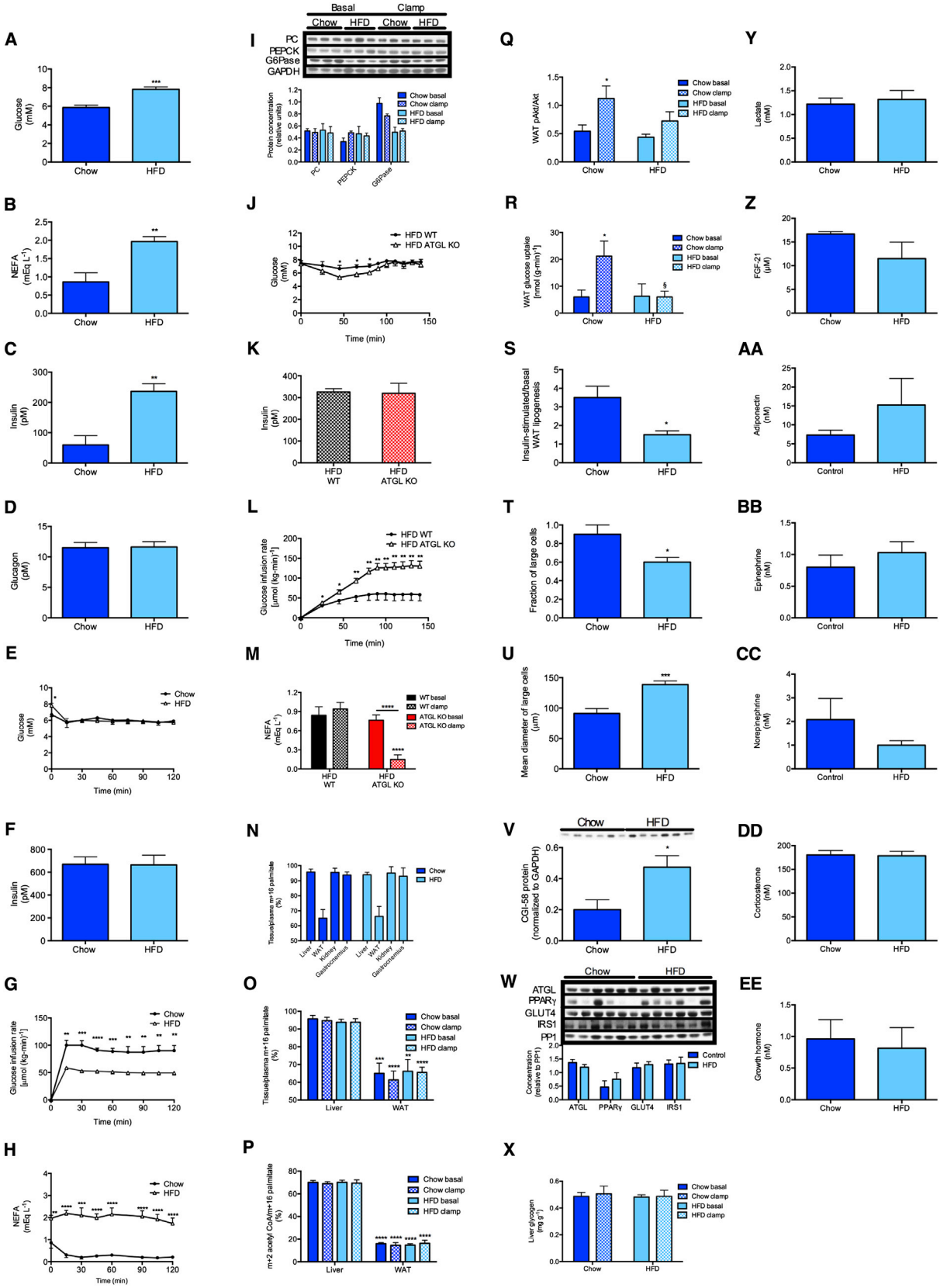


*(legend on next page)*

**Figure S4. Four Weeks of High Fat Feeding Increases Hepatic Glucose Production as a Result of Increased Lipolysis, Related to Figure 4**

(A–D) Plasma glucose, NEFA, insulin and glucagon concentrations. In all panels, *p < 0.05, **p < 0.01, ***p < 0.001, ****p < 0.0001.

(E) Plasma glucose during a hyperinsulinemic-euglycemic clamp.

(F) Plasma insulin at the end of the clamp.

(G) Glucose infusion rate.

(H) Plasma NEFA throughout the clamp.

(I) Liver gluconeogenic protein expression.

(J) Plasma glucose concentrations during a hyperinsulinemic-euglycemic clamp in ATGL knockout mice.

(K) Plasma insulin concentrations at the end of the clamp.

(L) Glucose infusion rate during the clamp.

(M) Plasma NEFA.

In (J–M), n = 8 per group.

(N) Ratio of tissue to plasma $^{13}C_{16}$ palmitate in four tissues in rats infused with [U-$^{13}C_{16}$] palmitate.

(O) Ratio of tissue to plasma $^{13}C_{16}$ palmitate in rats infused with [U-$^{13}C_{16}$] palmitate. Basal data were copied from (N).

(P) Ratio of $^{13}C_2$ acetyl CoA to $^{13}C_{16}$ palmitate in rats infused with [U-$^{13}C_{16}$] palmitate.

(Q) Akt phosphorylation in WAT.

(R) Glucose uptake in WAT.

(S) Insulin-stimulated lipogenesis in WAT.

(T) Fraction of large adipocytes.

(U) Mean diameter of large adipocytes.

(V) CGI58 protein in WAT.

(W) WAT protein expression.

(X) Liver glycogen content.

(Y) Plasma lactate.

(Z–EE) Plasma FGF-21, adiponectin, corticosterone, epinephrine, norepinephrine, and growth hormone concentrations. Unless otherwise specified, data are mean ± SEM of n = 6 per group, with comparisons by t test.

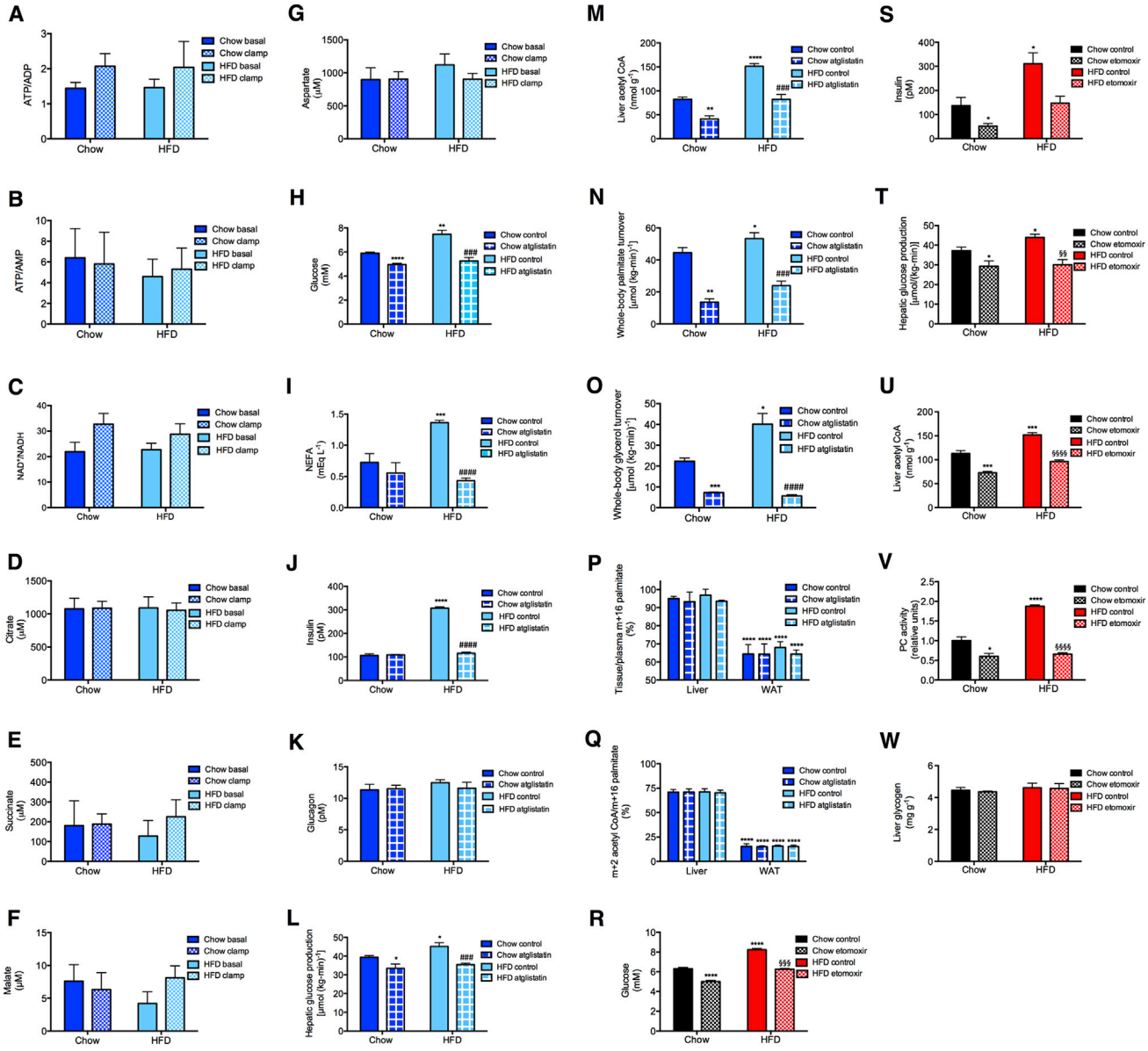


**Figure S5. Increased Lipolysis Causes Insulin Resistance in High-Fat-Fed Rats, Related to Figure 4**

(A–C) Ratios of ATP/AMP, ATP/ADP, and $NAD^+$/NADH in liver. In all panels, *p < 0.05, **p < 0.01, ***p < 0.001, ****p < 0.0001 versus chow fed, control rats; ##p < 0.01, ###p < 0.001, ####p < 0.0001 versus HFD, control rats by the 2-tailed unpaired Student's t test.

(D–G) Liver citrate, succinate, malate, and aspartate concentrations.

(H–K) Fasting plasma glucose, NEFA, insulin, and glucagon concentrations in rats treated with atglistatin.

(L) Hepatic glucose production.

(M) Liver acetyl CoA content.

(N and O) Whole-body palmitate and glycerol turnover.

(P) Ratio of tissue to plasma $^{13}C_{16}$ palmitate in rats infused with [U-$^{13}C_{16}$] palmitate.

(Q) Ratio of $^{13}C_2$ acetyl CoA to $^{13}C_{16}$ palmitate in rats infused with [U-$^{13}C_{16}$] palmitate.

(R and S) Fasting plasma glucose and insulin in rats treated with etomoxir.

(T) Hepatic glucose production.

(U) Liver acetyl CoA.

(V) PC activity.

(W) Liver glycogen.

In (R–W), *p < 0.05, ***p < 0.001, ****p < 0.0001 versus chow fed controls, §§ p < 0.01, §§§ p < 0.001, §§§§ p < 0.0001 versus high fat fed controls by the 2-tailed unpaired Student's t test. Data are mean ± SEM of n = 6 per group, with comparisons by t test.

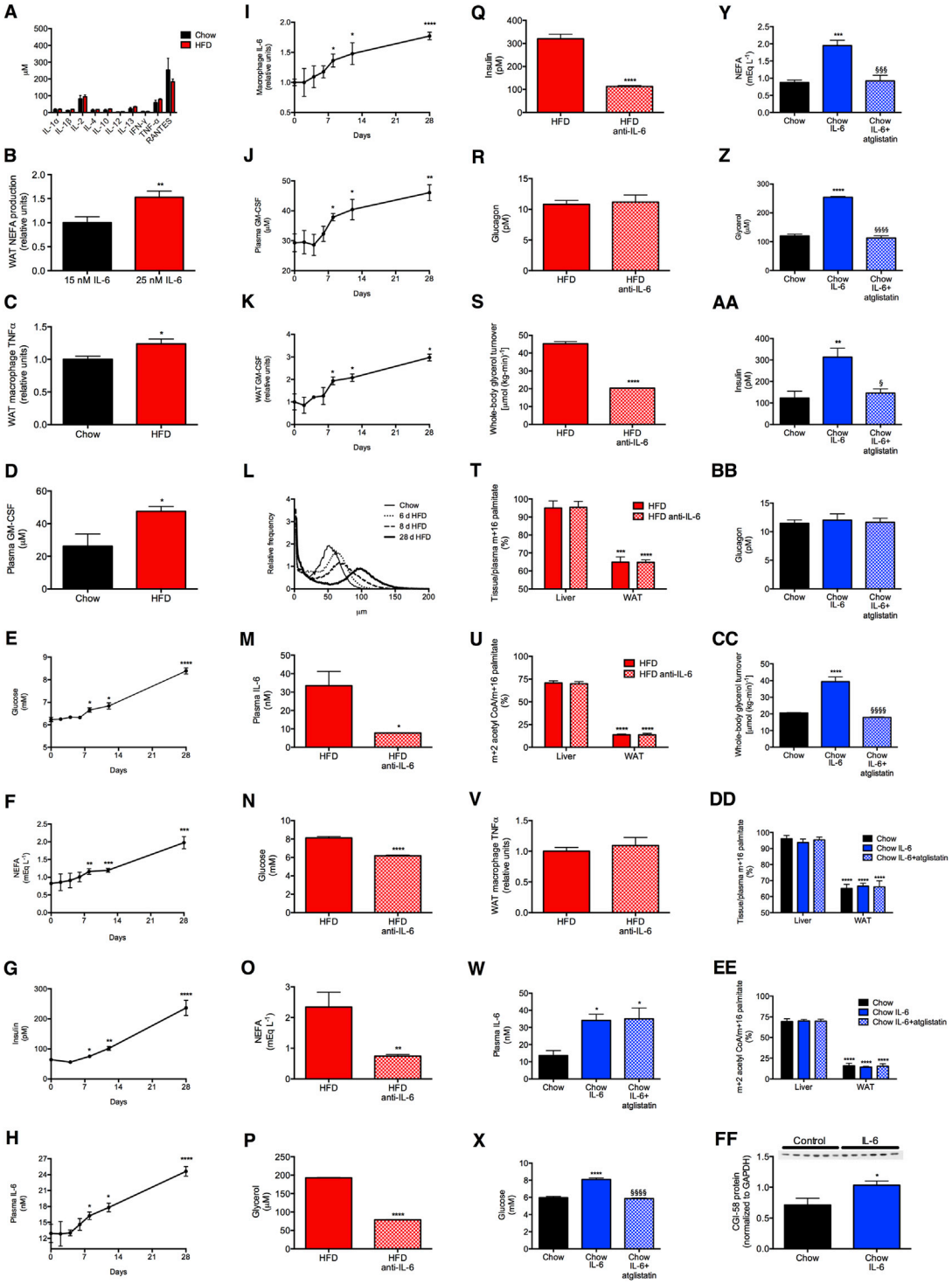


**Figure S6. Increases in Plasma IL-6 Cause Increased Lipolysis and Hyperglycemia in High-Fat-Fed Rats, Related to Figure 5**

(A) Inflammatory cytokine concentrations.

(B) WAT NEFA production over 24 hr.

(C) Plasma granulocyte macrophage colony stimulating factor concentrations.

(D) WAT macrophage TNFα concentrations. In (A–D), *$p < 0.05$, **$p < 0.01$ by the 2-tailed unpaired Student's t test.

(E–G) Fasting plasma glucose, NEFA, and insulin concentrations after 2-28 days of high fat diet.

(H and I) Plasma and WAT macrophage IL-6 concentrations.

*(legend continued on next page)*

(J and K) Plasma and WAT GM-CSF concentrations.
(L) Cell size frequency distributions.
In (E–L), n = 4-8 per time point; *p < 0.05, **p < 0.01, ***p < 0.001, ****p < 0.0001 versus day 0 by the 2-tailed unpaired Student's t test.
(M–R) Plasma IL-6, glucose, NEFA, glycerol, insulin, and glucagon concentrations in high fat fed rats treated with an IL-6 neutralizing antibody.
(S) Whole-body glycerol turnover.
(T) Ratio of tissue to plasma $^{13}C_{16}$ palmitate in rats infused with [U-$^{13}C_{16}$] palmitate.
(U) Ratio of $^{13}C_2$ acetyl CoA to $^{13}C_{16}$ palmitate in rats infused with [U-$^{13}C_{16}$] palmitate.
(V) WAT macrophage TNF$\alpha$. In (M–V), *p < 0.05, **p < 0.01, ***p < 0.001, ****p < 0.0001 by the 2-tailed unpaired Student's t test.
(W–BB) Plasma IL-6, glucose, NEFA, glycerol, insulin, and glucagon concentrations in rats treated with an intra-arterial infusion of IL-6 with or without pre-treatment with atglistatin.
(CC) Whole-body glycerol turnover.
(DD) Ratio of tissue to plasma $^{13}C_{16}$ palmitate in rats infused with [U-$^{13}C_{16}$] palmitate.
(EE) Ratio of $^{13}C_2$ acetyl CoA to $^{13}C_{16}$ palmitate in rats infused with [U-$^{13}C_{16}$] palmitate.
(FF) WAT CGI-58 concentrations.
In (W)-(FF), *p < 0.05, **p < 0.01, ***p < 0.001, ****p < 0.0001 versus chow fed rats; § p < 0.05, §§ p < 0.01, §§§ p < 0.001, §§§§ p < 0.0001 versus IL-6 infused rats by by ANOVA with Bonferroni's multiple comparisons test. Unless otherwise stated, data are mean ± SEM of n = 6 per group.

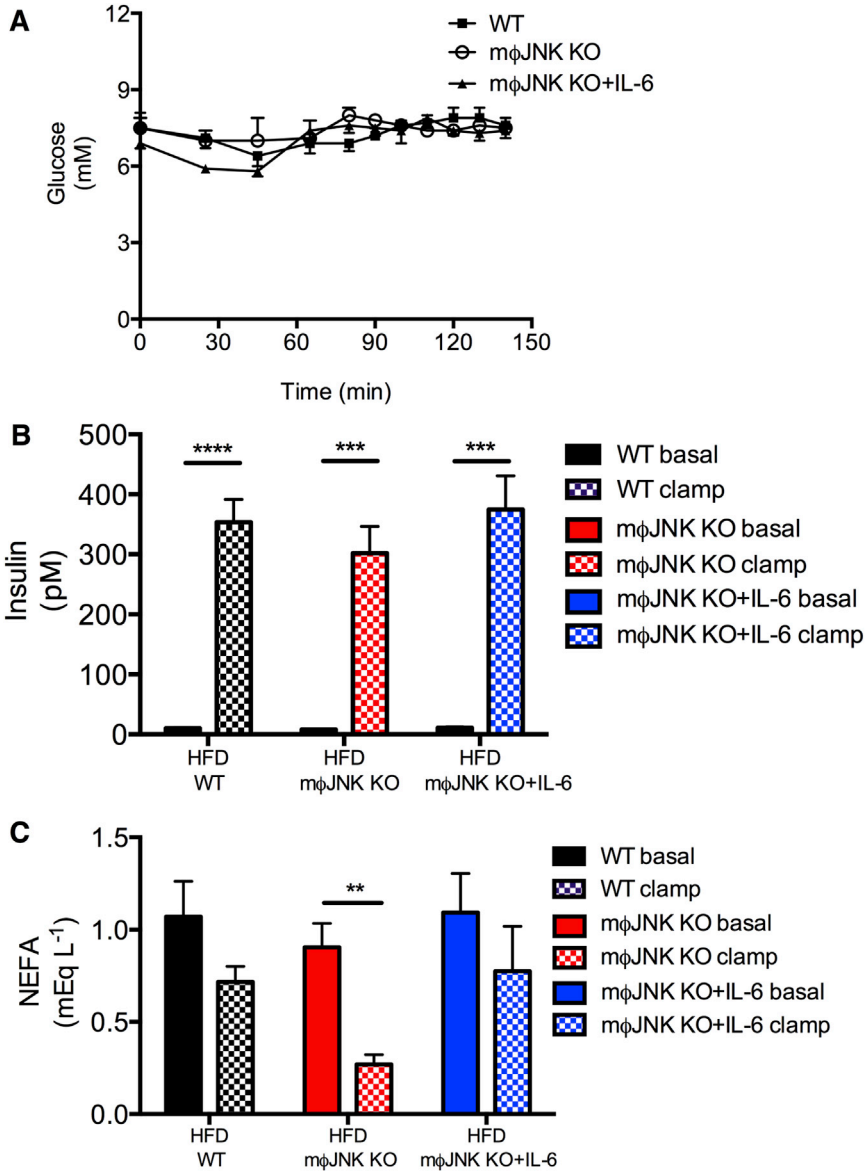


**Figure S7. Mice Lacking JNK in Macrophages Are Protected from Diet-Induced Hepatic Insulin Resistance, Related to Figure 6**

(A) Plasma glucose concentrations during the hyperinsulinemic-euglycemic clamp.

(B) Plasma insulin concentrations.

(C) Plasma NEFA.

**p < 0.01, ***p < 0.001. Data are mean ± SEM of n = 10 (WT), 8 (mϕJNK KO) or 10 (mϕJNK KO+IL-6) per group. Comparisons were performed by ANOVA with Bonferroni's multiple comparisons test.